Electronic Supplementary Material (ESI) for Physical Chemistry Chemical Physics.

Supplementary Information for

Simulating polyhedral formation of fullerene precursor

Benjamin Heuser,[a,b] Kurt V. Mikkelsen,[c] and James E. Avery[d]

This PDF file includes:

Overview of Supplementary Information
Figs. S1 to S23

[a] Niels Bohr Institute, University of Copenhagen, Blegdamsvej 17, 2100 Copenhagen Ø, E-mail: krn362@alumni.ku.dk
[b] Helmholtz-Zentrum Dresden-Rossendorf, Bautzner Landstraße 400, 01328 Dresden, Germany
[c] Department of Chemistry, University of Copenhagen, Universitetsparken 5, 2100 København Ø, E-mail: kmi@chem.ku.dk
[d] Niels Bohr Institute and DIKU, University of Copenhagen, Blegdamsvej 17, 2100 Copenhagen Ø, E-mail: avery@nbi.ku.dk

Supporting Information

The closing of the precursor molecule was performed with the two halogens fluorine and chlorine. For the choice of fluorine, an additional path was calculated, in which the initial geometry for all geometry optimisations had the fluorine and hydrogen atoms in the inmost cavity rotated to the inside. The remaining atoms were in the exact same positions as for the path, in which the fluorine and hydrogens were placed outside. Although the initial geometries differ, the same atoms were allowed to be optimised during the calculations. This means, that after the geometry optimisation procedure is finished, the atoms' positions depend on their initial placement. For some of the calculations the initial placement on the inside of the carbon cage resulted in a geometry of higher energy then an initial placement on the outside. This can be seen as a local minimum with higher energy.

An illustration of the two different input geometries for the outside and the inside path is displayed in figure S1.

The following sections show the same plots as in the article, first for the choice of chlorine as a halogen and then for the path, where fluorine has been placed on the inside of the molecule.

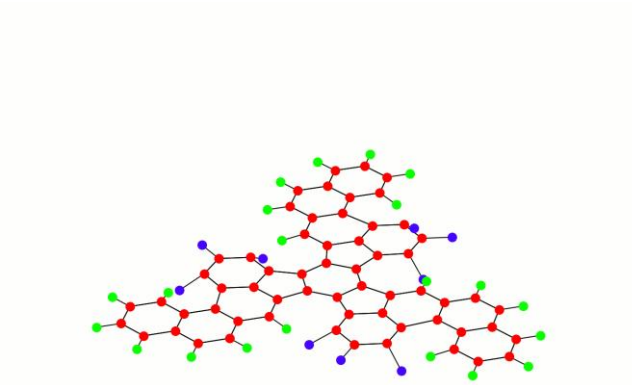

(a) Outside path 1

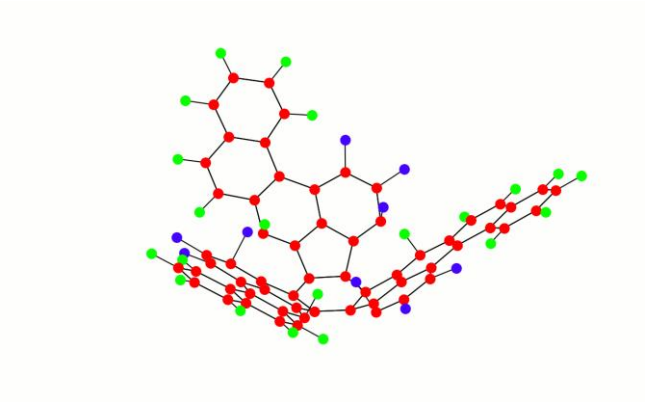

(b) Inside path 1

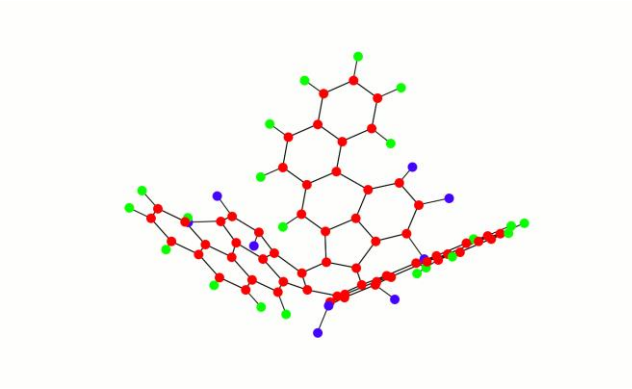

(c) Outside path 2

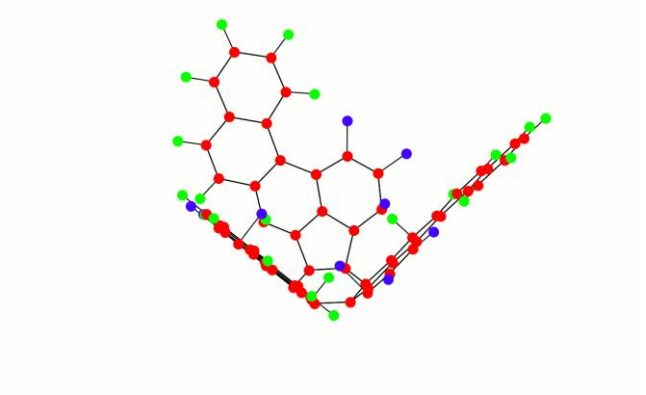

(d) Inside path 2

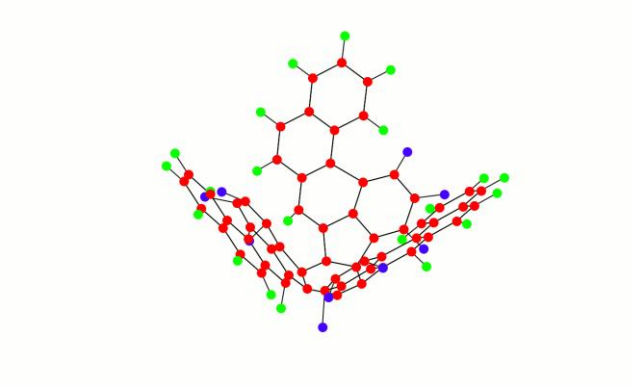

(e) Outside path 3

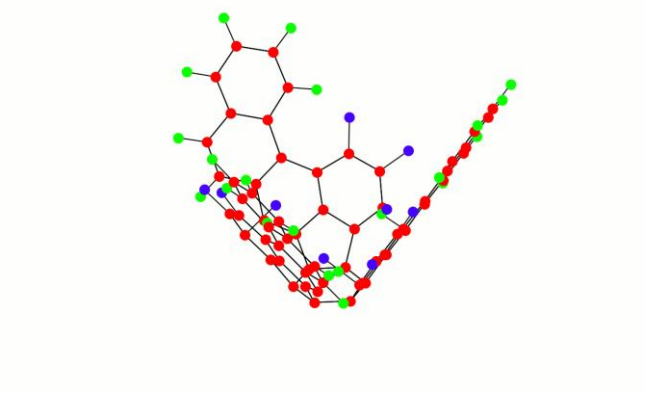

(f) Inside path 3

Fig. S1. Illustration of the input geometries for the outside (left) and the inside (right) path

1. Optimised Geometries of the Chlorinated Precursor Molecule

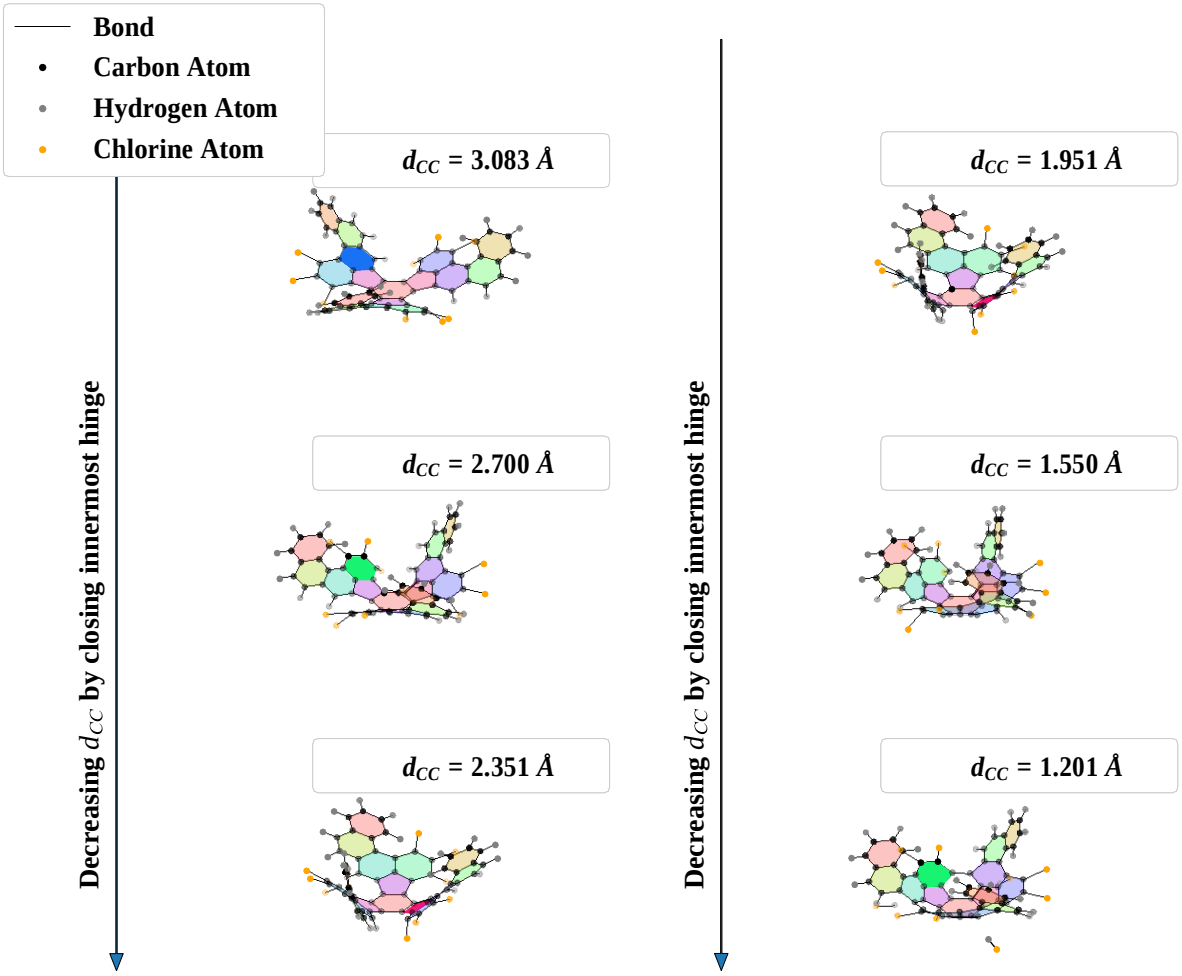

Fig. S2. Optimised geometries for the C_{60} precursor molecule with chlorine in key positions, sampled as a function of the carbon carbon distance.

2. Fluorinated Precursor Molecule taking the Outside Path

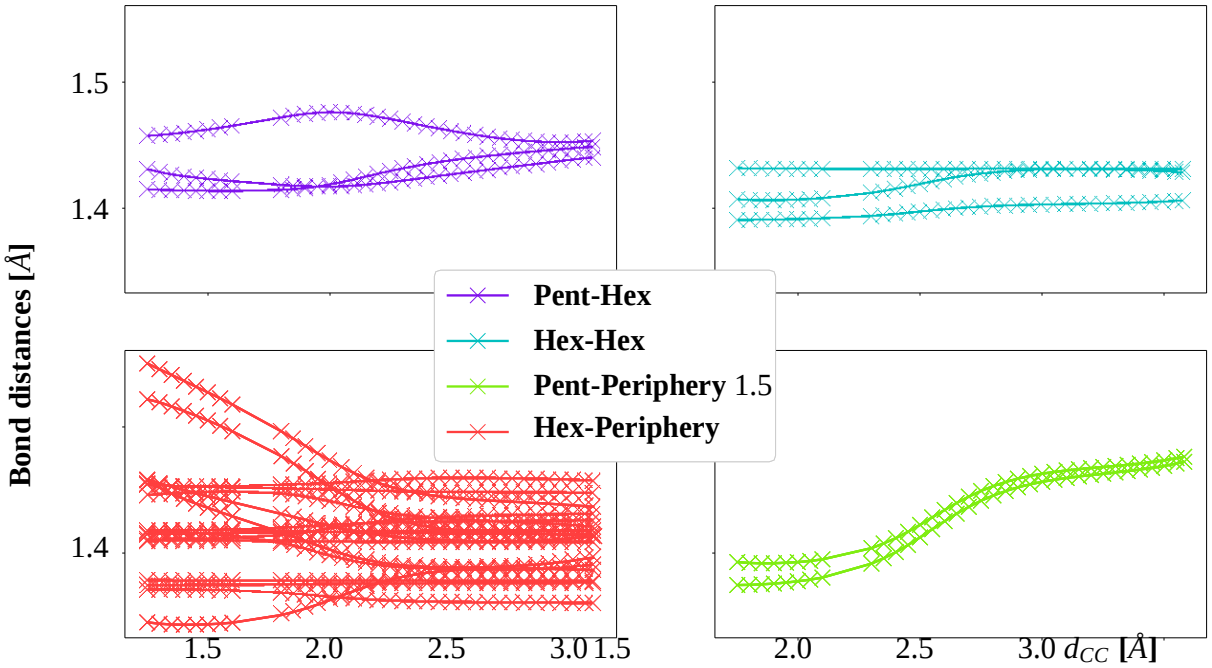

Fig. S3. Development of the four different types of bond lengths in the C_{60} precursor molecule along the auto-assembly path with H and F placed outside of the forming sphere.

3. Chlorinated Precursor Molecule taking the Outside Path

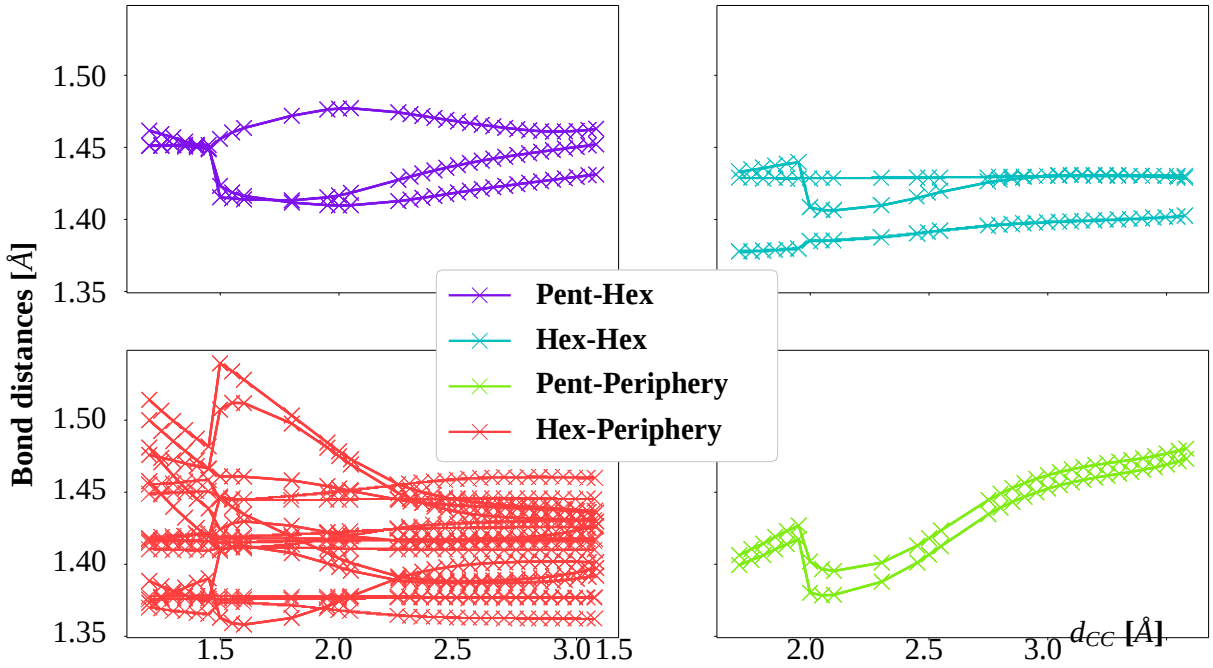

Fig. S4. The four different bond types which occur in the chlorinated C_{60}-Ih precursor molecules as a function of the carbon-carbon distance.

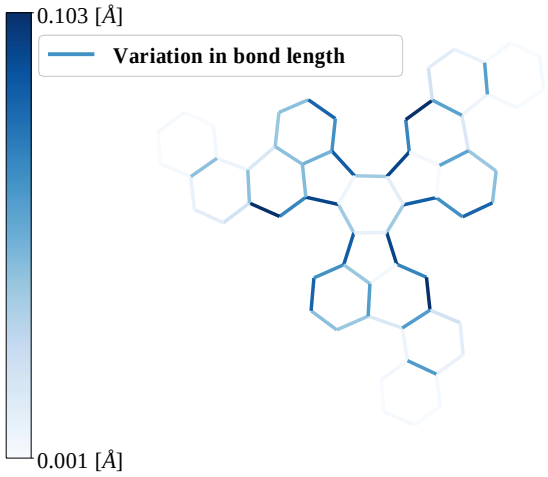

(a) Maximal variation of the bond lengths along the path.

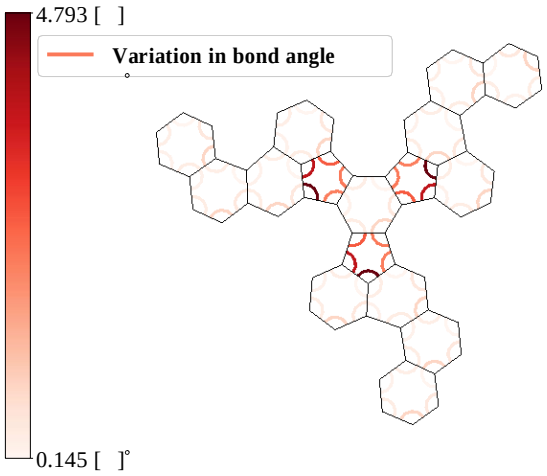

(b) Maximal variation of the bond angles along the path.

Fig. S5. Maximal absolute difference of bond lengths and angles along the outside closing path for the chlorinated precursor molecule.

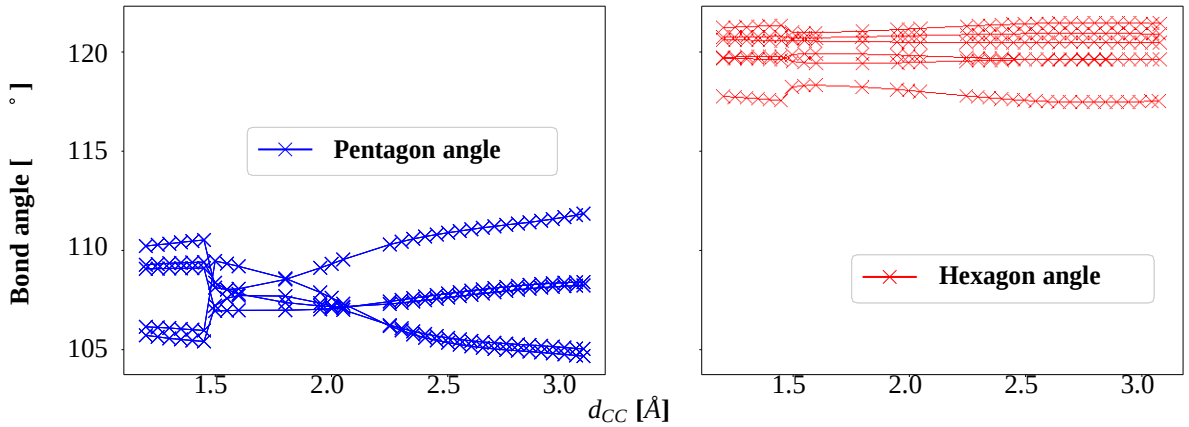

Fig. S6. Development of angles within pentagon and hexagon faces along the outside closing path for the chlorinated precursor molecule.

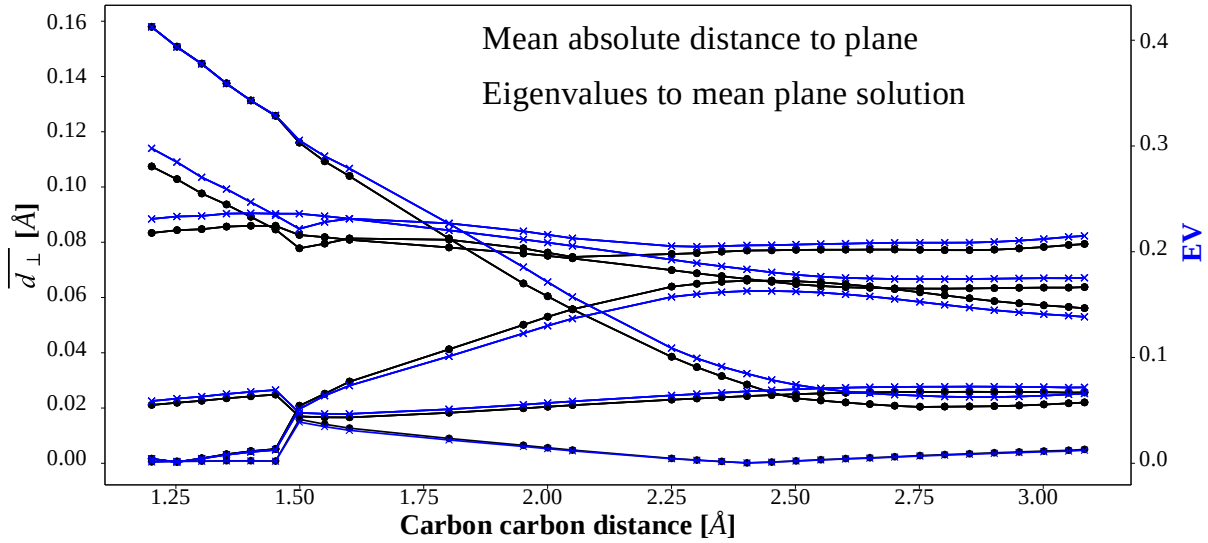

Fig. S7. Development of the face planarity in terms of mean distance from the plane and described by the smallest eigenvalue of the least squares problem for the chlorinated precursor molecule and outside reaction path.

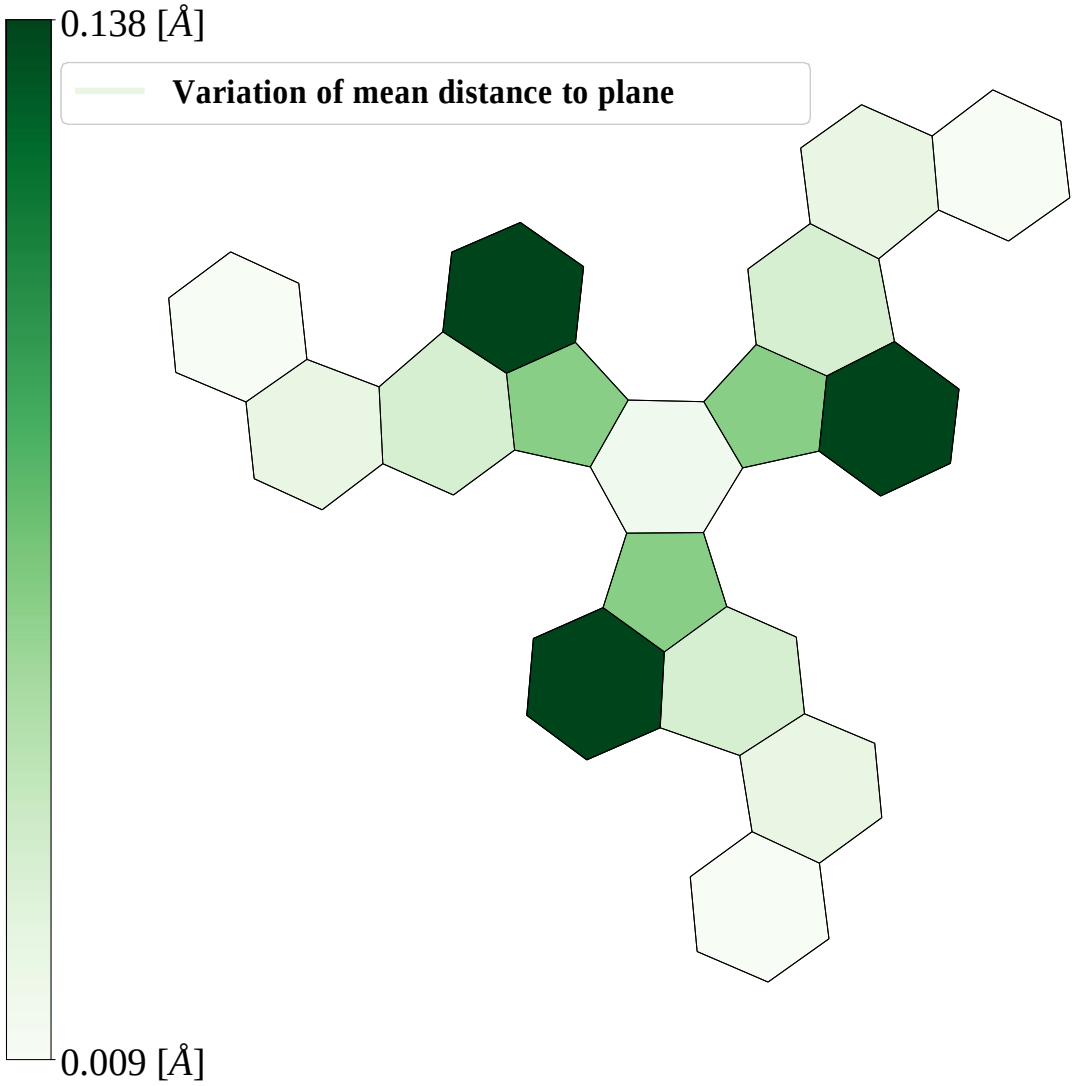

Fig. S8. Range of the mean absolute distance of all vertices of a face from the mean plane along the outside closing path with chlorine.

4. Chlorinated Precursor Molecule during the second Carbon-Carbon Bond Formation

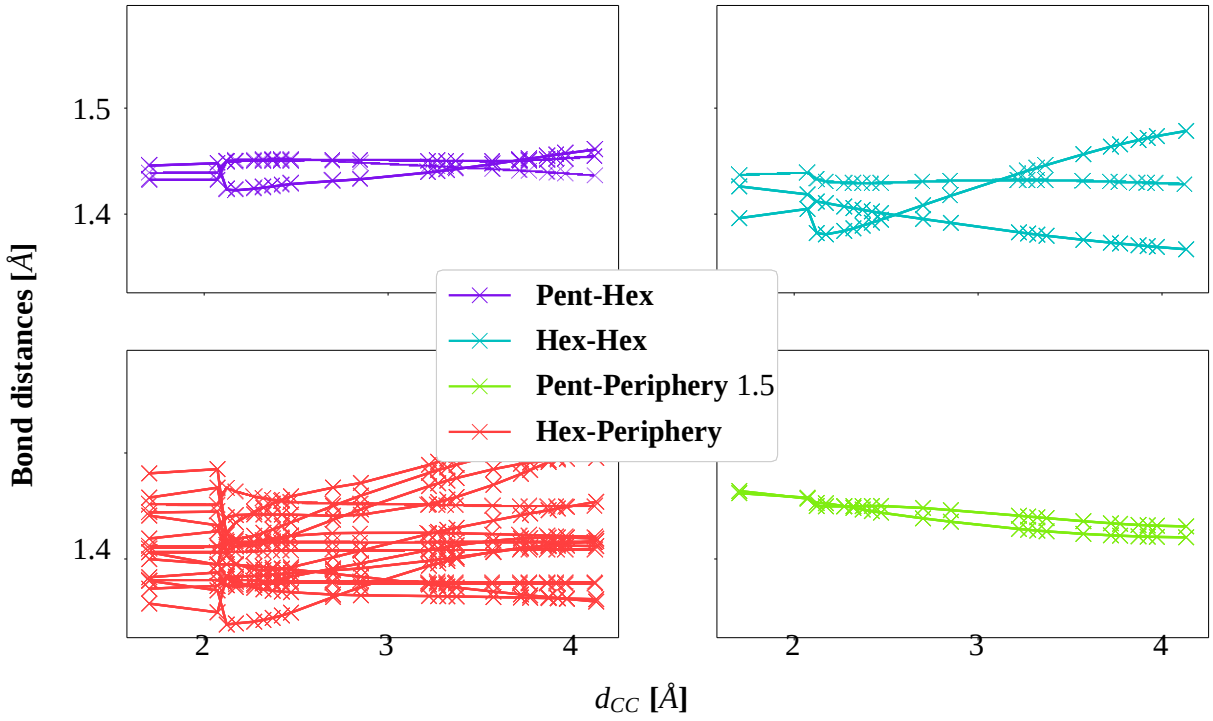

Fig. S9. The four different bond types which occur in the chlorinated C_{60}-Ih precursor molecules as a function of the carbon-carbon distance, during the second carbon-carbon bond formation.

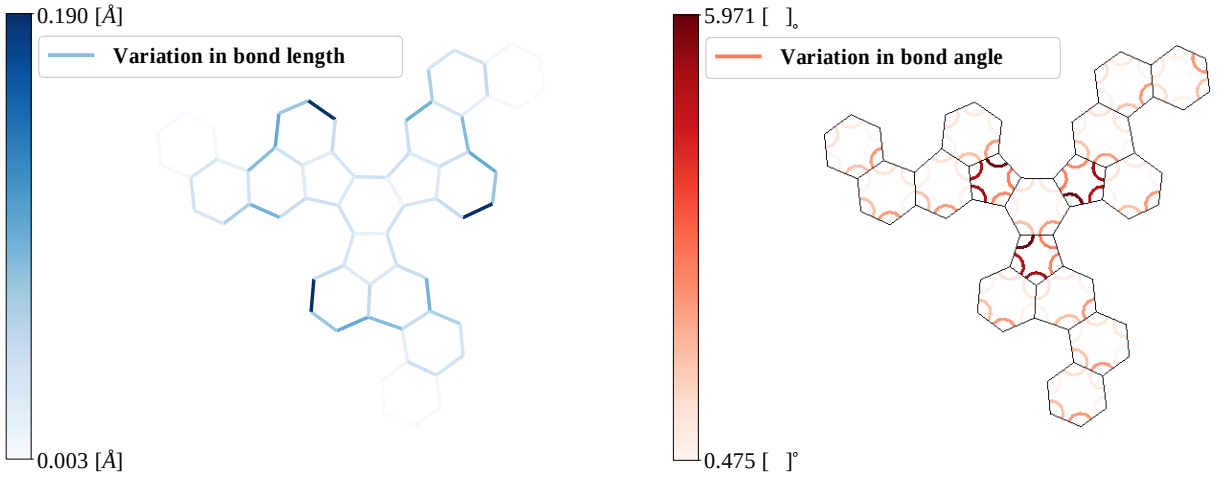

(a) Maximal variation of the bond lengths along the path. (b) Maximal variation of the bond angles along the path.

Fig. S10. Maximal absolute difference of bond lengths and angles along the outside closing path for the chlorinated precursor molecule at the second carbon-carbon bond formation.

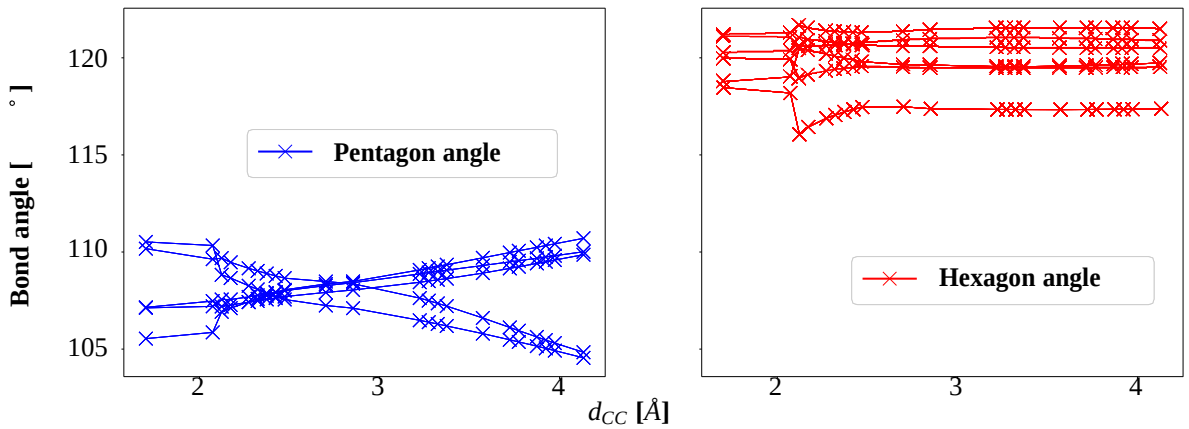

Fig. S11. Development of angles within pentagon and hexagon faces along the outside closing path for the chlorinated precursor molecule, during the second carbon-carbon bond formation.

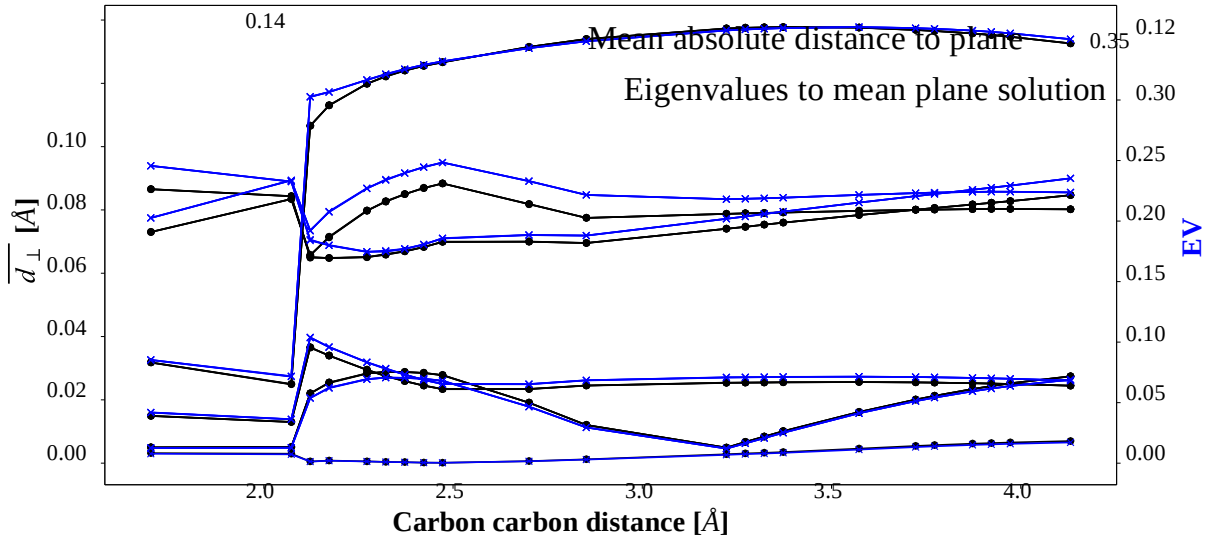

Fig. S12. Development of the face planarity in terms of mean distance from the plane and described by the smallest eigenvalue of the least squares problem for the chlorinated precursor molecule and outside reaction path, during the second carbon-carbon bond formation.

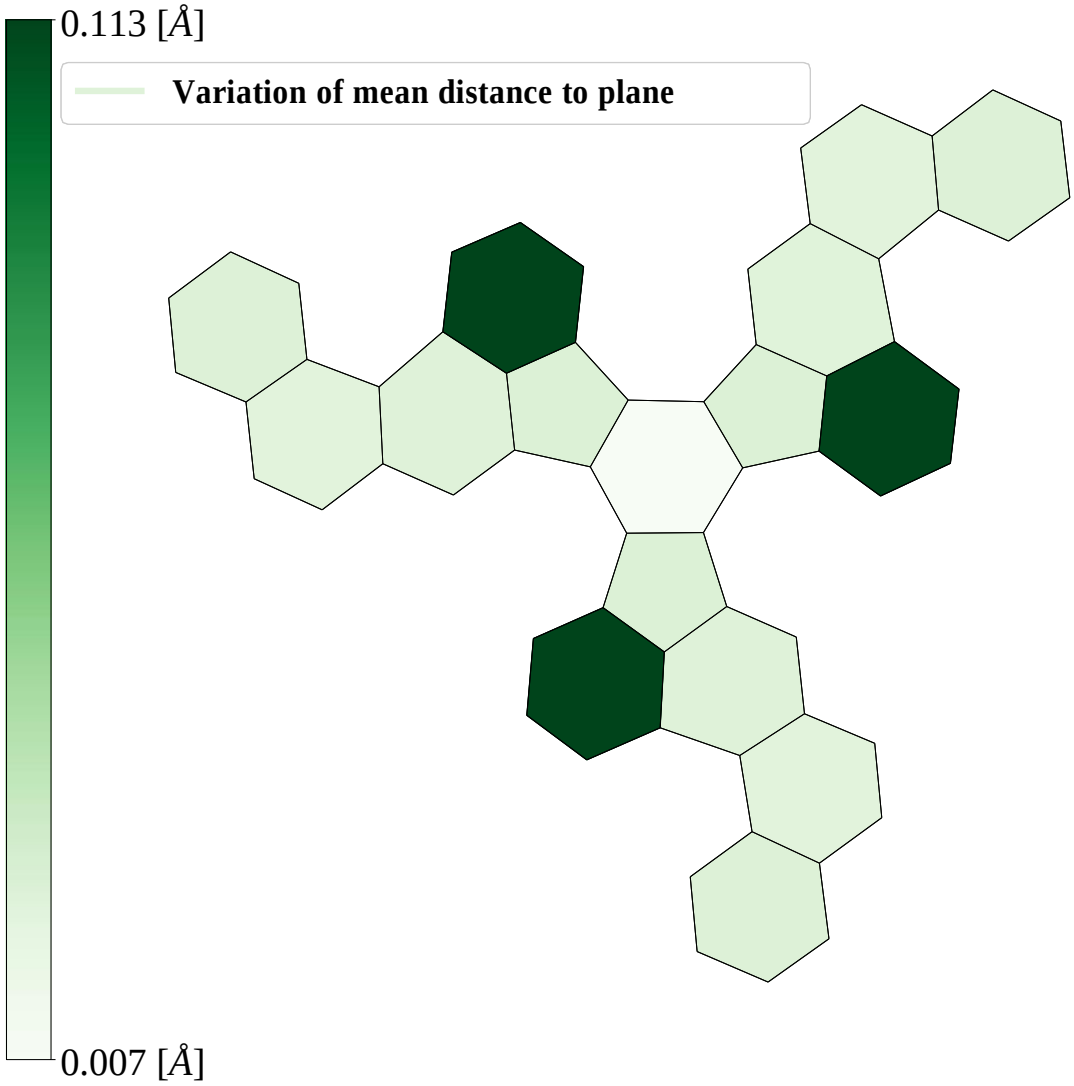

Fig. S13. Range of the mean absolute distance of all vertices of a face from the mean plane along the outside closing path with chlorine, during the second carbon-carbon bond formation.

5. Chlorinated Precursor Molecule during the third Carbon-Carbon Bond Formation

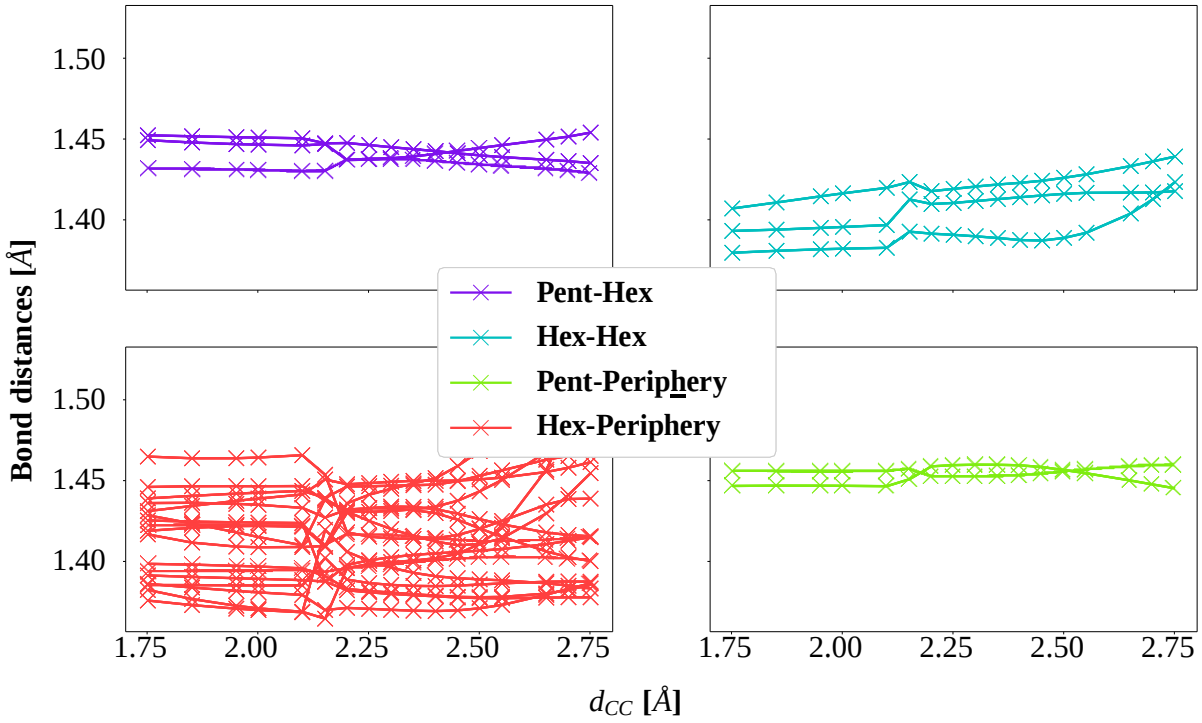

Fig. S14. The four different bond types which occur in the chlorinated C_{60}-Ih precursor molecules as a function of the carbon-carbon distance, during the third carbon-carbon bond formation.

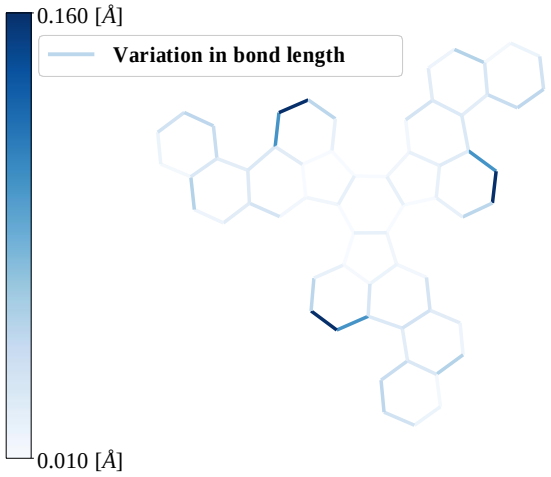

(a) Maximal variation of the bond lengths along the path.

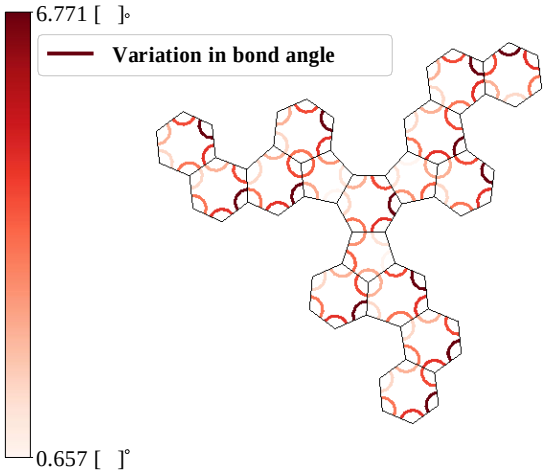

(b) Maximal variation of the bond angles along the path.

Fig. S15. Maximal absolute difference of bond lengths and angles along the outside closing path for the chlorinated precursor molecule at the third carbon-carbon bond formation.

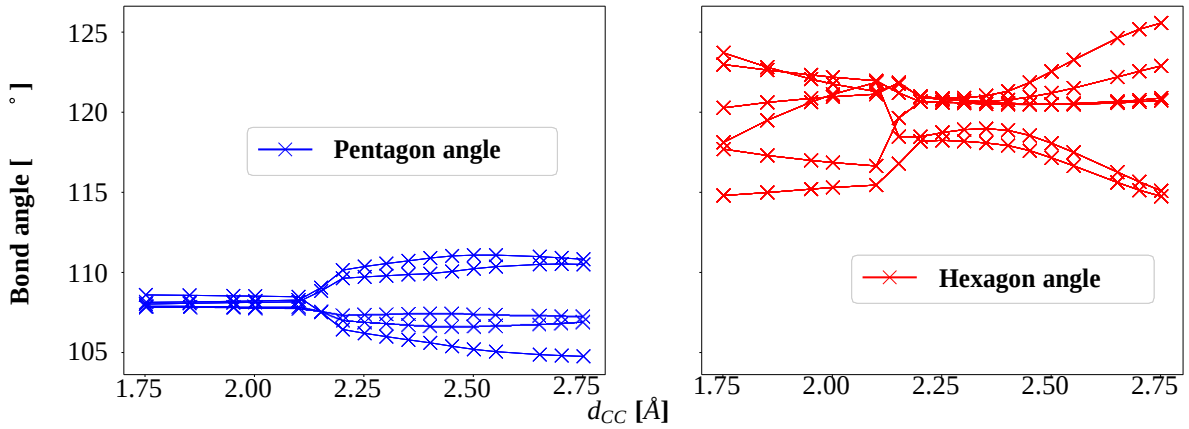

Fig. S16. Development of angles within pentagon and hexagon faces along the outside closing path for the chlorinated precursor molecule, during the third carbon-carbon bond formation.

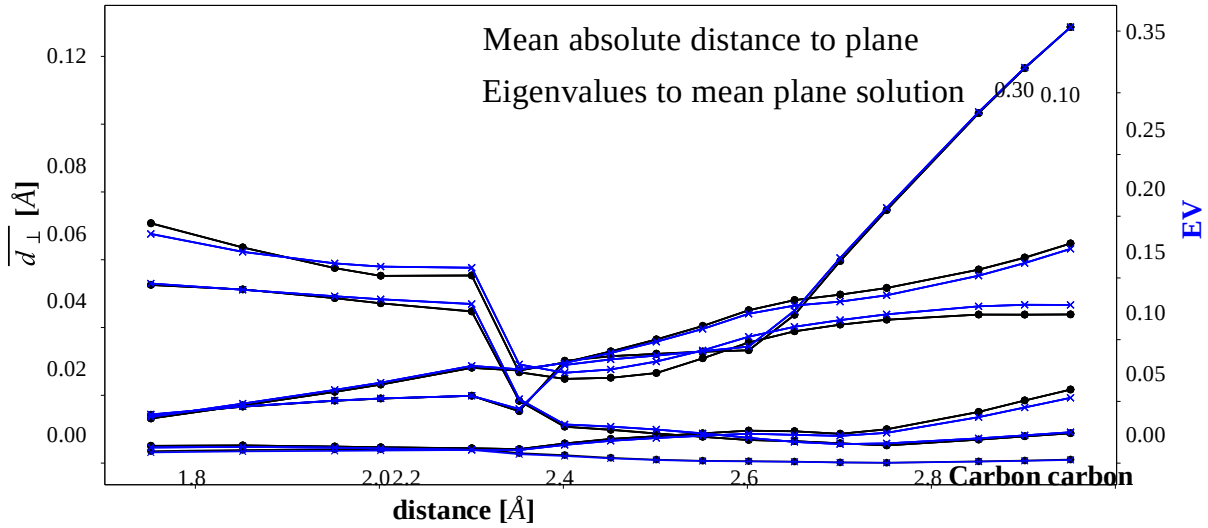

Fig. S17. Development of the face planarity in terms of mean distance from the plane and described by the smallest eigenvalue of the least squares problem for the chlorinated precursor molecule and outside reaction path, during the third carbon-carbon bond formation.

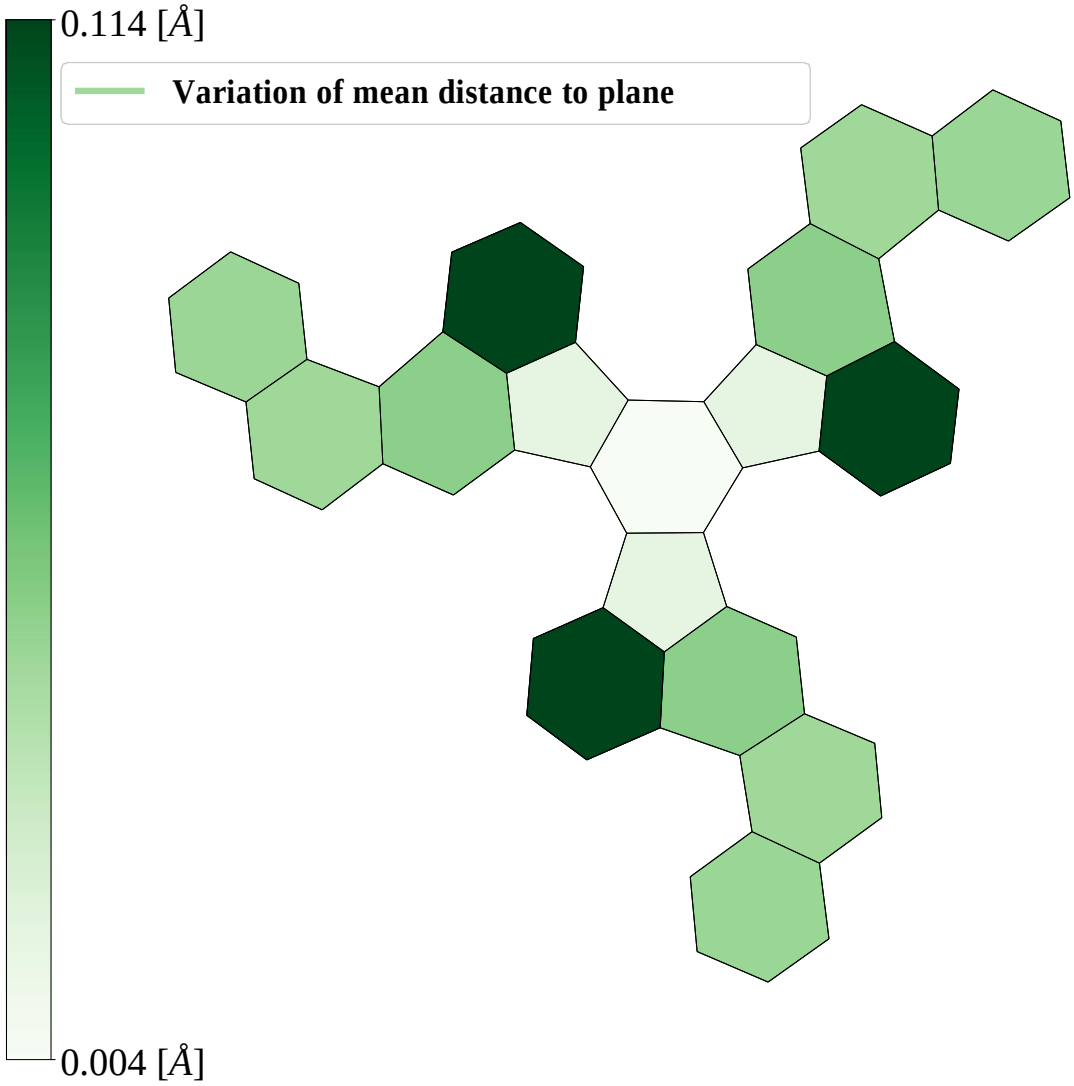

Fig. S18. Range of the mean absolute distance of all vertices of a face from the mean plane along the outside closing path with chlorine, during the third carbon-carbon bond formation.

6. Fluorinated Precursor Molecule taking the Inside Path

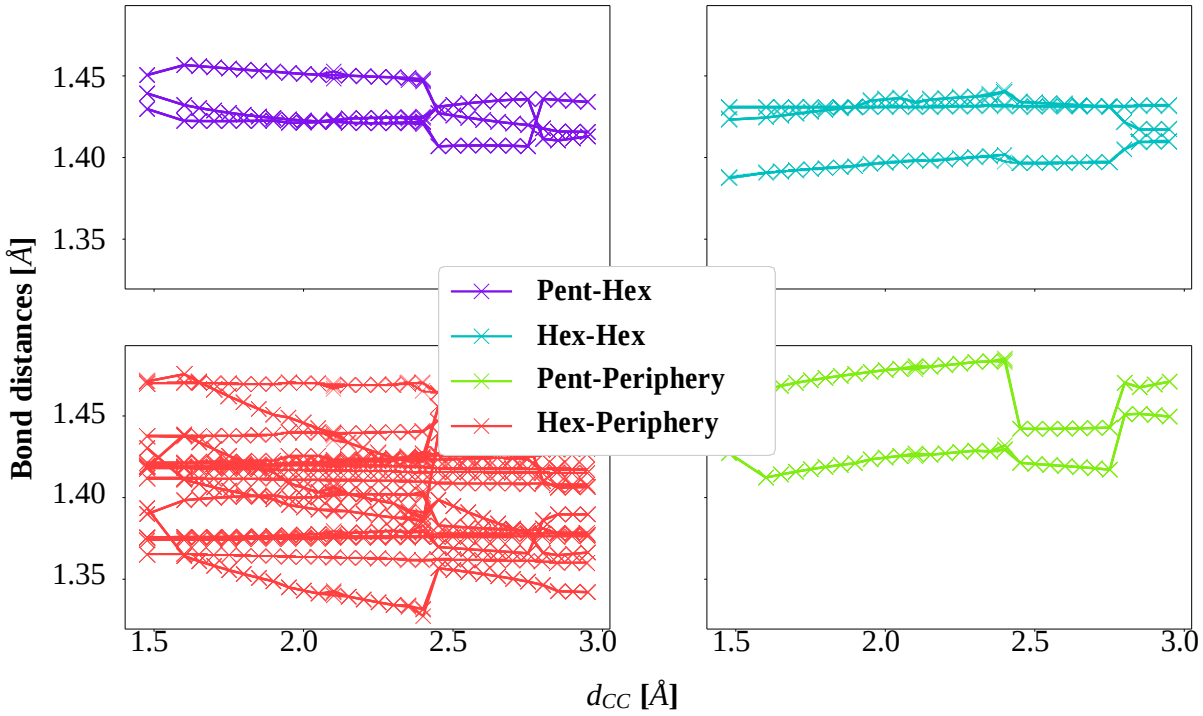

Fig. S19. The four different bond types which occur in the fluorinated C_{60}-Ih precursor molecules, taking the reaction path with the F and H atoms placed on the inside, as a function of the carbon-carbon distance.

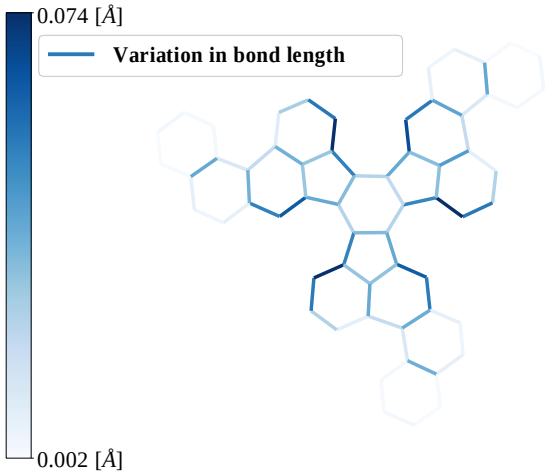

(a) Maximal variation of the bond lengths along the path.

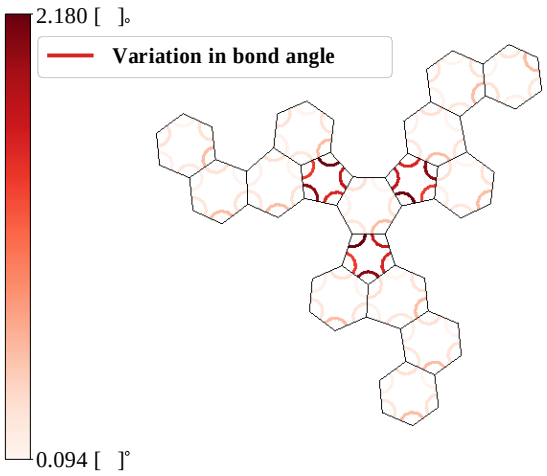

(b) Maximal variation of the bond angles along the path.

Fig. S20. Maximal absolute difference of bond lengths and angles along the inside closing path for the fluorinated precursor molecule.

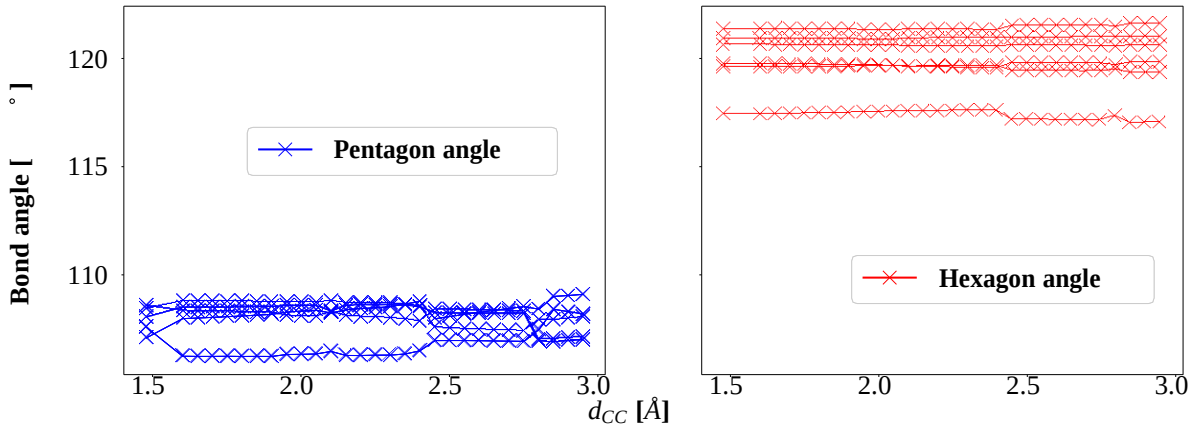

Fig. S21. Development of angles within pentagon and hexagon faces along the inside closing path for the fluroinated precursor molecule.

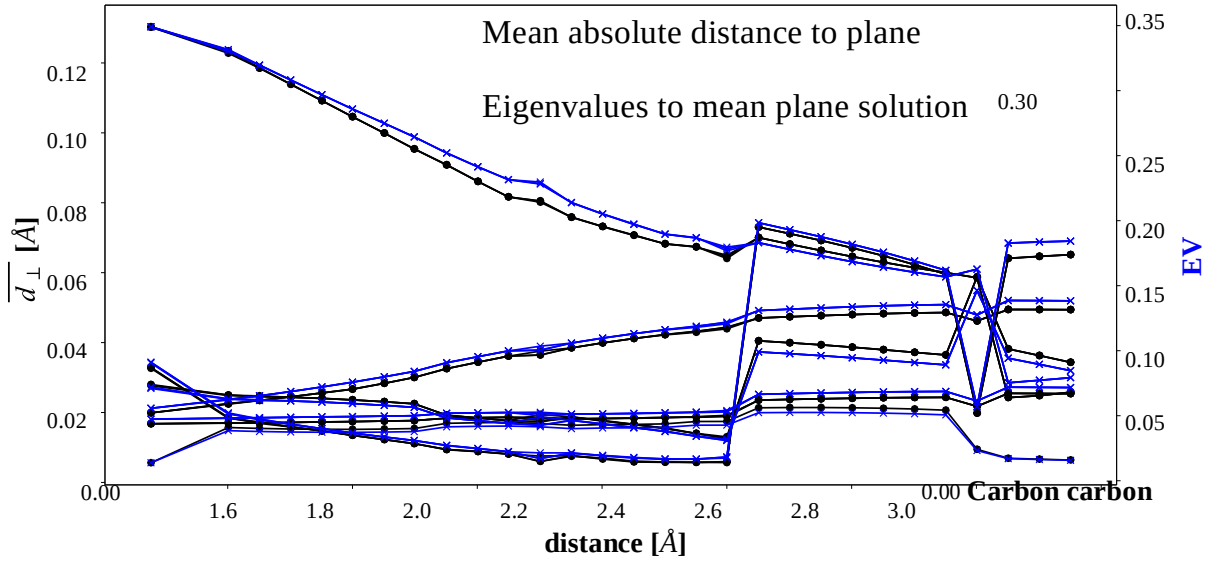

Fig. S22. Development of the face planarity in terms of mean distance from the plane and described by the smallest eigenvalue of the least squares problem for the fluorinated precursor molecule and inside reaction path.

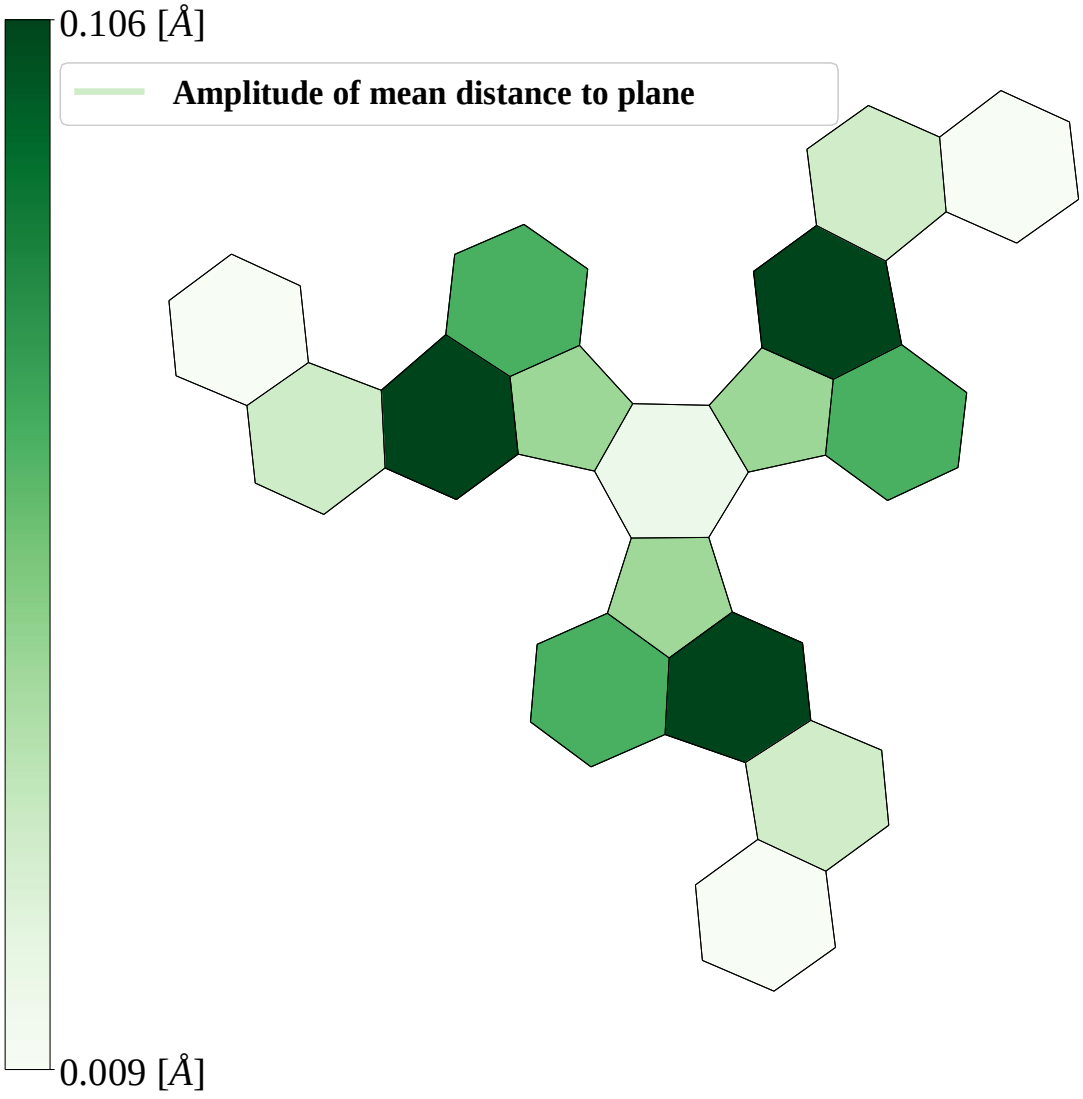

Fig. S23. Range of the mean absolute distance of all vertices of a face from the mean plane along the inside closing path with fluorine.